Electrochimica Acta 342 (2020) 136071

Contents lists available at ScienceDirect

Electrochimica Acta

journal homepage: www.elsevier.com/locate/electacta

Formation of benzyl viologen-containing films at copper and their protective properties

Ursula Carragher , Carmel B. Breslin *

Department of Chemistry, Maynooth University, Maynooth, Co. Kildare, Ireland

ARTICLE INFO

Article history:
Received 6 December 2019
Received in revised form
13 March 2020
Accepted 13 March 2020
Available online 18 March 2020

Keywords:
Benzyl viologen
Copper
Corrosion protection
Adsorbed viologens
Protective viologen films

ABSTRACT

Benzyl viologen (BV) was deposited at copper in the presence of chloride anions to generate a benzyl viologen-chloride layer at copper, where the viologen was present as a dication, stabilised by the negatively charged chloride anions. This layer provided good protective properties to the underlying copper substrate. On polarising the BV-modified copper in 0.1 M NaCl significantly lower currents, typically 28 μA cm^{-2}, were observed at 0.40 V vs SCE compared to the higher currents of 1.75 mA cm^{-2} evident with the unmodified copper. The charge-transfer resistance at −0.15 V vs SCE, obtained from impedance data recorded in 0.1 M NaCl after 60 min, was measured as 21 kΩ cm^2 for copper indicating the build-up of corrosion products, while a lower resistance of 8 kΩ cm^2 was seen with the BV-modified copper. The estimated chloride content at the copper surface following immersion in chloride solutions was reduced from about 22% to 4% on modification with BV. Less protective properties were observed when the benzyl viologen was deposited from oxalate, sulfate and acetate solutions, and when the benzyl viologen was replaced with methyl or ethyl viologens, illustrating the importance of the supporting anions and viologen compound. The reduction of the di-cationic BV^{2+} to the radical cation was observed at −0.57 V vs SCE, while the further reduction of the radical species was seen at −0.73 V vs SCE, indicating that the deposited benzyl viologen exhibits its characteristic redox properties.

1. Introduction

Viologens, also known as 1,1′-disubstituted 4,4′-bipyridinium ions, are widely studied as electron transfer mediators in enzymatic reactions [1,2]. Other successful applications include electrochromic materials and photochemical devices for solar energy conversion [3,4]. The electrochemistry of viologen compounds in solution has been studied in detail [5,6]. The dicationic viologen undergoes a reversible one electron reduction to give a radical cation. This radical cation is normally soluble but with large substituents bound to the pyridilium nitrogen, the radical species may deposit onto the electrode. In the second electron transfer step, the radical cation undergoes a one electron transfer step to give the neutral viologen, which is frequently insoluble in aqueous media. The radical cations can also form dimers, or polymerisation of the radical species may occur.

Viologens are known to form ordered adsorbed layers at a variety of surfaces, including Au (111), Cu(100), Cu(111) and highly oriented pyrolytic graphite [7–16]. For example, Lee et al. [7] have studied the properties of assembled derivatives of viologens using electrochemical quartz microbalance (EQCM) measurements. Arihara et al. [8] monitored the adsorption of heptyl viologen on Au (111) using infrared reflection absorption spectroscopy and concluded that the di-cationic molecule adsorbs in a side-on orientation, but on reduction forms a face-on dimer composed of two mono-cations. Higashi et al. [9] used a combination of voltammetry, electro-reflectance and electrochemical scanning tunnelling microscopy to probe the influence of Cl^-, Br^- and F^- on the adsorption of benzyl viologen at Au(III). The observed formation of an ordered co-adsorption layer of viologen and Cl^- was attributed to electrostatic attractive interactions between the viologen and the Cl^- under-layer at the Au(III) surface. A non-faradaic order-disorder phase transition was observed at 0.30 V. Similar two-phase transitions were observed with Cl^- and Br^-, but not with F^-, and it was concluded that the specific adsorption of coexisting anions is important for the phase transition. There have also been some reports on the adsorption of viologens at copper and copper modified surfaces. Jiang et al. [10] have reported the potential-dependent adsorption of heptyl viologen on a Cu(100)

* Corresponding author.
E-mail address: Carmel.Breslin@mu.ie (C.B. Breslin).

https://doi.org/10.1016/j.electacta.2020.136071
0013-4686/

surface in a chloride-containing electrolyte. In the absence of the viologens, a highly ordered chloride adlayer was observed on the Cu(100). On addition of the viologen, an ordered two-dimensional array structure was observed as the di-cations assembled and adsorbed at the surface. The one electron reduction of the di-cations caused a phase transition to a stripe-like pattern, while the further reduction produced a more compact stripe phase. At lower applied potentials, an amorphous phase was observed. However, in the reverse anodic sweep, the reproduction of the ordered stacking phases was achieved on top of the chloride lattice at the Cu(100) surface. Breuer et al. [11] also studied the adsorption of dibenzyl and diphenyl viologens at chloride-modified copper. The dibenzyl viologens were adsorbed and stabilised at the chloride-modified copper in the di-cationic state. Electrostatic interactions between the anionic chloride layer and the di-cations were proposed as the main driving force for the formation of the stabilised layer. Again, a stripe-like structure of chains was observed on reduction of the layer. Tsay et al. [12] studied the molecular structures obtained on adsorption of dicarboxylated viologens on Cu(100) in the presence of chloride anions. Depending on the oxidation state of the viologen, array-like patterns, stripe patterns, compact stripe patterns, and metastable phases were observed. Hydrogen bonding was considered to be the main factor in achieving the close stacking stripe pattern. Pham et al. [13] studied the surface redox chemistry of adsorbed viologens on a chloride-modified Cu(100) surface. Again, the electrostatic interaction between BV^{2+} and the negatively charged chloride lattice was attributed to the formation of the adsorbed BV layer. Viologens have also been shown to adsorb in the absence of a chloride layer. Peterson et al. [17] studied the binding of methyl viologen to CdS quantum dots with a surface layer of oleic acid (OA). It was concluded that the methyl viologen adsorbed at the CdS through displacement of the weakly bound Cd-OA complex or by direct adsorption to the exposed CdS surface. It was suggested that the methyl viologen adsorbed with its bipyridyl core lying flat at the surface.

The antimicrobial and antibacterial properties of viologens are well known [18] and they have been employed to inhibit microbiologically induced corrosion [19]. An oxidised copper alloy, Cu–Ni, was modified with viologens to give good bacterial inhibition efficiency. A 4-(chloromethyl) phenyl trichlorosilane layer was first immobilised onto the oxidised Cu–Ni surface. Then, the viologen was coupled to this layer and the terminal pyridine groups were converted to pyridinium groups.

The purpose of this study was to determine if adsorbed viologen molecules have any corrosion protective properties. Polycrystalline copper was chosen as the adsorption of viologens at Cu(100) has been studied and the role of chloride anions in the formation and stabilisation of these layers is known. On the other hand, it is well known that copper is susceptible to corrosion and that chloride anions promote the dissolution of copper [20–23]. Therefore, adsorbed viologen layers were formed at polycrystalline copper in chloride, sulfate, oxalate and acetate containing solutions and the protective properties of these layers were evaluated. Additional studies were performed where the protective properties of benzyl, ethyl and methyl viologen adsorbed layers were compared. To the best of our knowledge, there are no reports in the literature that focus on the protective properties of these adsorbed viologen layers.

2. Experimental

The electrochemical deposition of the viologens was carried out using a CH Instruments 760C potentiostat. All measurements were made at room temperature with deionised water. A polycrystalline copper rod (4 mm diameter, 99.99%) obtained from Goodfellow was encased in a Teflon holder, and used as an electrode with an exposed geometric surface area of 0.1257 cm^2. The rod electrodes were polished using a 1 μm diamond polish and Buehler microcloth, sonicated to remove any polishing residue using a Branson 1510 sonicator and rinsed well with deionised water and dried under a stream of air to give a smooth surface finish. A saturated calomel electrode (SCE) was used as the reference electrode and a high surface area platinum wire was employed as the counter electrode. Unless otherwise stated, the viologen layers were formed in a quiescent chloride solution with 2.0 mM benzyl viologen (BV) by polarising the copper electrode from −0.20 V to 1.0 V vs SCE at 1 mV s^{-1}, after a 10 min immersion period in the solution. All solutions were purged with nitrogen to remove any traces of dissolved oxygen. The solution was adjusted to a pH of 3.0 using a few drops of HCl to prevent the formation of copper oxides/hydroxides. The modified copper was then removed and washed thoroughly before it was used in further experiments.

The protective properties of the deposited viologen films were studied in a neutral 0.1 M NaCl solution by polarising the electrodes from −0.20 V vs SCE at 1 mV s^{-1} until dissolution was observed. Tafel plots were recorded in the vicinity of the corrosion potential at 0.5 mV s^{-1}. Again, none of the solutions were stirred. The electrodes were immersed in 0.1 M NaCl for a 30-min period before polarisation. Electrochemical impedance spectroscopy was used to study the stability of the BV-modified copper electrodes in 0.1 M NaCl. The impedance was recorded at potentials from −0.15 V to 0.60 V vs SCE as a function of time. All data were recorded using a Solartron Model 1287 potentiostat coupled with a Solartron Model 1255 frequency response analyser. A potential perturbation of 5 mV was used to ensure a pseudo-linear response of the system, while the frequency was varied from 65 kHz to 10 mHz. Scanning electron micrographs (SEM) were obtained using a Hitachi FE-scanning electron microscope, with an Oxford instruments Inca X-act 4.12 software package, and EDX analysis was carried out using an EDX Model 51-ADD0009 with the software package Micro Analysis Suite, while a Emitech K550x gold sputter coater was used to produce thin films of gold at the samples for SEM analysis. The concentration of copper ions in solution was monitored using a spectrophotometric approach where a bathocuprione chelating agent ($C_{26}H_{20}N_2$) was used to generate an orange-coloured complex with Cu^{2+} ions. The absorbance of the complex was recorded at 480 nm using a Cary 50 UV–Visible spectrometer.

3. Results and discussion

3.1. Formation of the BV-containing films at copper

The viologen-containing films were formed on the copper surface in the presence of different supporting electrolytes by cycling the electrode at 1 mV s^{-1} from an initial potential of −0.20 V vs SCE to a final potential of 1.0 V vs SCE in 2.0 mM BV. Representative plots are shown in Fig. 1, where the voltammograms recorded in the presence and absence of BV are compared using chloride, oxalate, acetate and sulfate as the supporting electrolytes. In all cases lower currents are observed in the viologen-containing solutions. In the viologen-free chloride solution, Fig. 1(a), the current increases with increasing potential to reach values of about 1.1 mA cm^{-2} at 0.40 V vs SCE and then fluctuates as the potential is cycled to higher values, indicating considerable dissolution of the copper substrate. This electrochemical behavior is consistent with the dissolution of copper and the nucleation of copper oxides, hydroxides and chloride-containing species, such as CuCl and the soluble $CuCl_2^-$ species [20–23]. Although not shown on the figure, the voltammograms recorded for copper in NaCl showed considerable

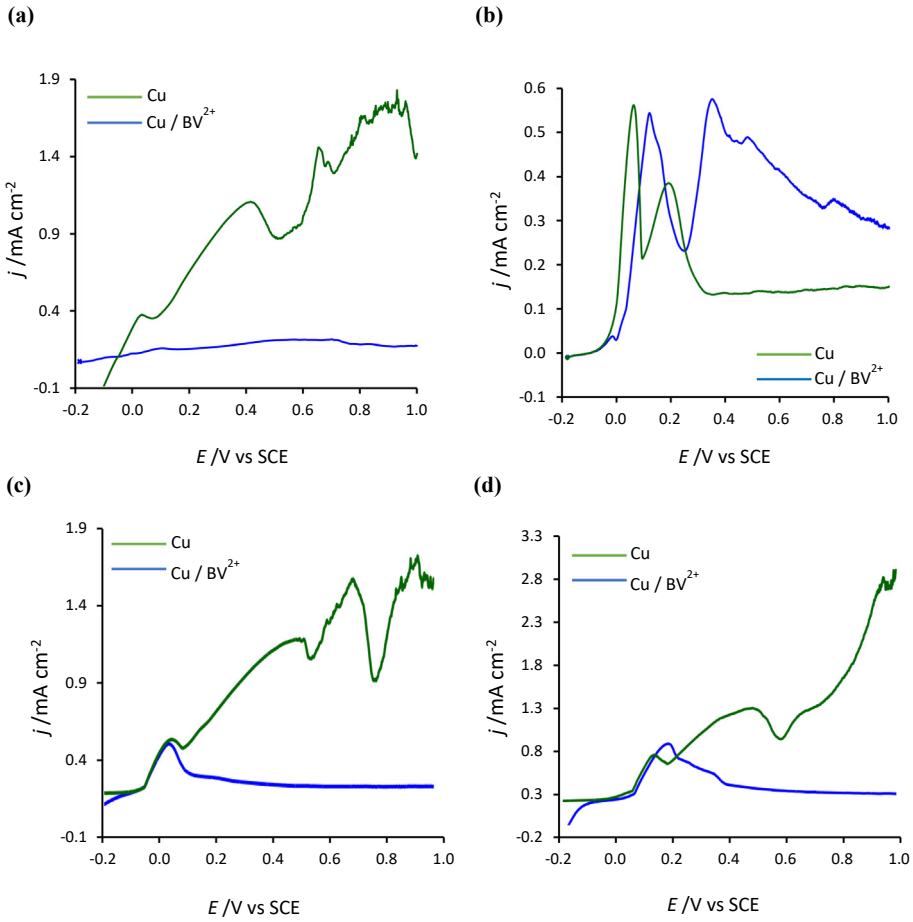

Fig. 1. Voltammograms recorded at 1.0 mV s^{-1} for copper in the presence of 2.0 mM BV (blue trace) and in the absence of BV (green trace) at a pH of 3.0 in **(a)** 0.1 M NaCl **(b)** 0.10 M $Na_2C_2O_4$ (c) 0.1 M CH_3COONa and (d) 0.1 M Na_2SO_4.

variation, as the substrate corroded and corrosion products, both soluble and insoluble, were formed. The data recorded in the presence of BV are very different and there is very little evidence for the dissolution of copper. The initial dissolution peak at about 0.10 V vs SCE, is considerably smaller and this is followed by a pseudo−passive region that extends to 1.0 V vs SCE. This indicates that the benzyl viologen is adsorbed onto the surface and this is sufficient to inhibit the dissolution of the copper electrode.

The formation of an insoluble copper oxalate film is clearly evident in Fig. 1(b). The currents are considerably lower than that observed in the chloride system. Dissolution of copper begins at about −0.05 V vs SCE and continues until a sufficient concentration of Cu^{2+} ions are formed to give rise to the formation of Cu−Ox complexes [24–26], Eqs. (1) and (2). It appears that in the presence of BV, the rate of formation of this Cu−Ox complex is inhibited somewhat. The initial dissolution peak appears at 0.15 V vs SCE, to give an approximate 100 mV shift in the peak potential and this may be related to the adsorption of the viologen, making the initial dissolution more difficult. However, once dissolution begins, the rapid decay in the current, seen in the absence of the viologen, is no longer evident and dissolution occurs for a longer period to give a broader peak and a slower rate of the copper-oxalate deposition at the surface.

$$Cu \rightarrow Cu^{2+} + 2e^{-} \quad (1)$$

$$Cu^{2+} + C_2O_4^{2-} + H_2O \rightarrow CuC_2O_4 + H_2O \quad (2)$$

The data shown for the acetate and sulfate systems show more significant dissolution of the copper substrate in the presence of the viologen, with initial peak currents of approximately 0.55 mA cm^{-2} and 0.95 mA cm^{-2} for the acetate and sulfate systems, respectively. Moreover, the initial dissolution event extends to about 0.40 V vs SCE with the viologen in the presence of sulfate. However, good stability is observed at the higher potentials. Considering the four systems, it is clear that the viologen film is more readily formed in the presence of chloride anions, while more complex dissolution and film formation events are evident in the oxalate and acetate systems, while the viologen films are slower to form in the presence of the larger sulfate anion.

The surface morphologies of the copper cycled in the absence and presence of the BV from −0.20 V to 0.60 V vs SCE are shown in the micrographs presented in Fig. 2(a) and (b), while the BV-containing films formed in the presence of oxalate and sulfate are shown in Fig. 2(c) and (d). There is little difference between the morphology in the absence and presence of the BV for the chloride system. However, leaf-like structures are clearly formed in the presence of the viologen. These are somewhat less developed in the simple chloride-containing solution. A rough layer with cracks is observed with the oxalate system, while the micrograph obtained with the sulfate system shows evidence of cracks and the deposition of corrosion products. Again, these data are consistent with the more efficient formation of the BV film at copper in the presence of chloride anions and this is in good agreement with the observations made by Breuer et al. [11] where dibenzyl and diphenyl viologens

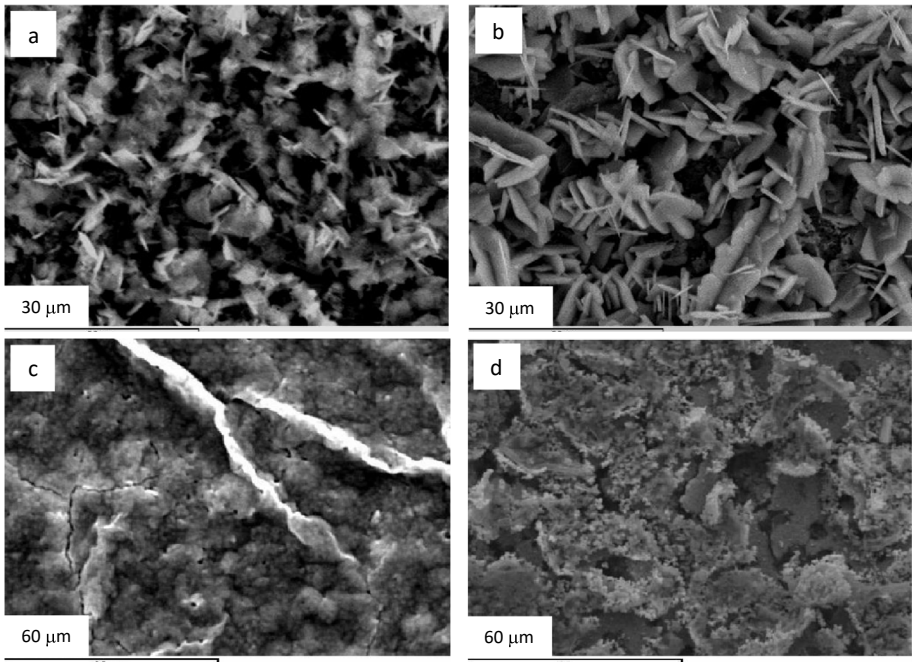

Fig. 2. Scanning electron micrographs recorded for copper cycled in **(a)** 0.1 M NaCl, **(b)** 0.1 M NaCl with 2.0 mM BV, **(c)** 0.1 M $Na_2C_2O_4$ with 2.0 mM BV and **(d)** 0.1 M Na_2SO_4 with 2.0 mM BV.

were adsorbed and stabilised at a chloride-modified copper in the di-cationic state.

As the chloride anions are essential in the formation of the stabilised BV film, the influence of the chloride concentration on the formation of the viologen films was studied. The chloride concentration was varied, while the concentration of the viologen was maintained at 2.0 mM and the pH of the final solution was maintained at a pH of 3.0. Representative data are shown in Fig. 3(a) where the data recorded in BV in the presence of 25 mM and 0.30 M NaCl are compared. At 0.30 M NaCl, relatively sharp peaks are observed, indicating the deposition of a stable CuCl complex, in a relatively short period, that facilitates the deposition of the viologen. However, at these higher concentrations, the formation of various soluble copper-chloride species, such as $CuCl_2^-$, $CuCl_3^{2-}$ and $CuCl_4^{3-}$, is possible [23]. The peak current is clearly dependent on the concentration of the chloride anion and increases to approximately 1 mA cm^{-2} in the presence of 0.30 M NaCl. At the lower 0.025 M NaCl concentration, the initial dissolution is shifted to higher potentials and occurs over a greater potential range, extending from 0.05 V to approximately 0.40 V vs SCE, indicating a slower rate of formation of the BV-containing films. It appears that 0.10 M is the more suitable chloride electrolyte, Fig. 1(a). At this concentration, the formation of the CuCl layer is efficient, but the chloride anion concentration is not sufficiently high to convert the CuCl layer to the soluble $CuCl_2^-$, $CuCl_3^{2-}$ and $CuCl_4^{3-}$ species. The influence of the nature of the viologen is summarised in the inset in Fig. 3(a), where charge is plotted as a function of potential for copper polarised in 0.1 M NaCl with 2.0 mM BV, EV (ethyl viologen) or MV (methyl viologen). While all three viologens reduce the rate of dissolution of the copper substrate, more protective properties are evident with BV and the charge remains low throughout the experiment. This may be related to the aromatic phenyl rings in the BV, facilitating the formation of a more compact and protective film.

The pH of the solution was varied as the pH will influence the surface with Cu_2O, CuO and hydrated copper oxides forming at the higher pH values. Moreover, it is well known that OH^- adsorption is facilitated at higher pH values to give passivation of the copper surface [20]. The influence of the pH is shown in Fig. 3(b), where the charge consumed to a potential of 0.40 V vs SCE is shown as a function of the pH. The higher charges in the acidic solutions are associated with a higher copper dissolution peak, while the increasing charge in the more alkaline solutions is consistent with the slower formation of the BV-chloride layer and the resulting higher currents seen from about 0.15 V to 0.40 V vs SCE. These data indicate that the BV layer forms more readily at slightly acidic or neutral conditions where copper oxides are not formed in large amounts. As the BV exists as the di-cation species, BV^{2+}, under these conditions, the BV layer can be represented as $([BV^{2+}2Cl^-]_nCuCl)$ where the initial CuCl facilitates the formation of the BV layer. This is in good agreement with studies on the formation of viologens at Cu(100) [10–13], where adsorbed chloride anions provide electrostatic interactions with the BV^{2+} to give a stable film. Variations in the initial potential from −0.50 V to −0.20 V vs SCE had no influence on the formation of the BV layer. Furthermore, the initial immersion of the copper in the BV-containing chloride solution for periods ranging between 30 s and 30 min had no influence on the formation of the BV-layer. It appears that the BV layer is generated once an initial chloride deposit is formed and this chloride layer is formed readily.

Although it is well known that EDX is only a qualitative technique, a quantitative analysis was carried out to give approximate information on the composition of the films. The copper was cycled from −0.50 V vs SCE to upper potentials of −0.20 V, 0.20 V and 0.60 V vs SCE. The EDX analyses were repeated several times, on different samples and at different points on the surface. Very good reproducibility was obtained, indicating uniform coverage of the copper. The intensities of the Cl and C were recorded and used to give approximate compositions. These data are summarised in Table 1, where the n value gives the number of samples analysed. At least five points on each sample were analysed. There is a considerable difference in the chloride content when the copper is cycled in the chloride and BV-containing chloride solutions. At −0.20 V vs SCE, only low amounts of the CuCl complex are formed in both

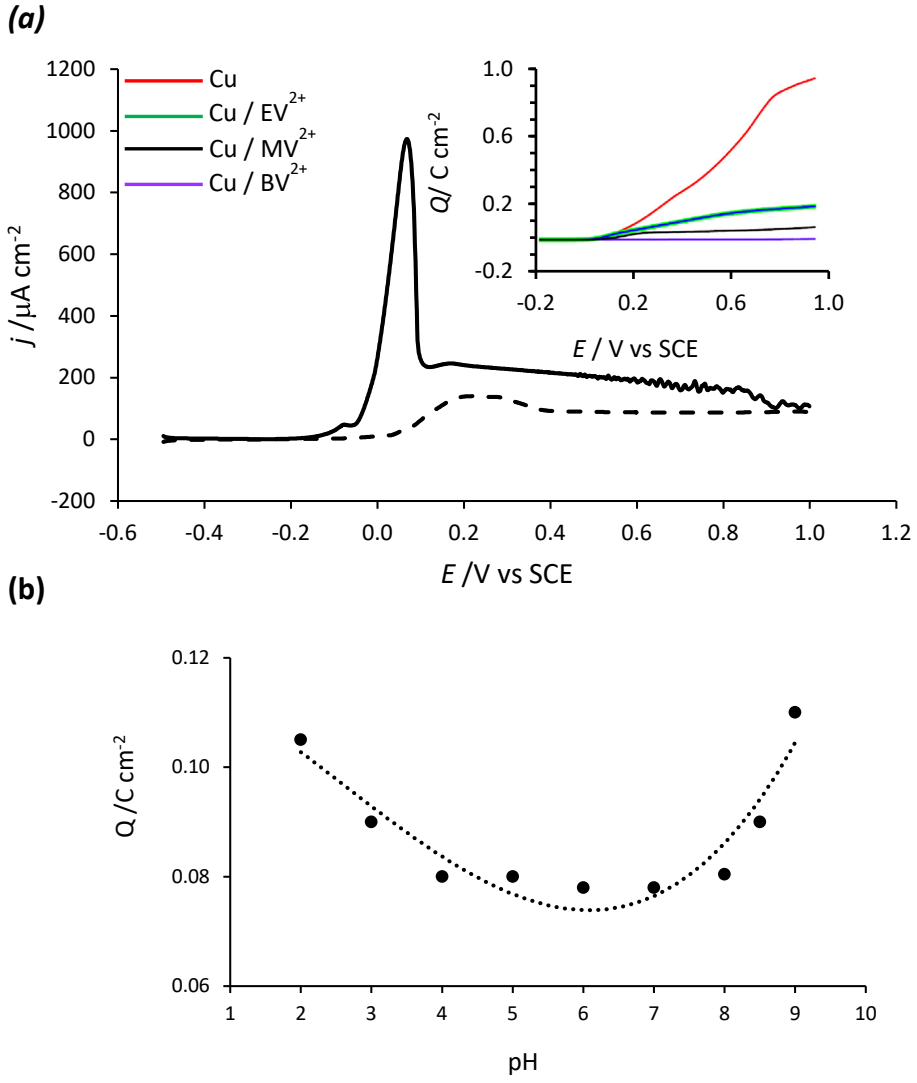

Fig. 3. **(a)** Voltammograms recorded at 1.0 mV s^{-1} for copper in 2.0 mM BV at a pH of 3.0 in ▬ ▬ ▬ 0.025 M NaCl and ▬▬ 0.30 M NaCl, inset: charge-potential plot for pure copper (red trace), EV-modified copper (green trace), MV-modified copper (black trace) and BV modified copper (purple trace) **(b)** charge as a function of pH on polarising copper in 2.0 mM BV in 0.1 M NaCl.

Table 1
EDX analysis of copper and BV-modified copper cycled to different upper potentials in 0.1 M NaCl at a pH of 3.0 (n = 10).

System	Potential/V vs SCE	%Cl	%C	$[Cu^{2+}]$/µM
Cu	−0.2	0.32 ± 0.1	–	3.75 ± 0.15
	0.2	22.3 ± 5.1	–	4.29 ± 0.20
	0.6	22.5 ± 4.5	–	4.88 ± 0.22
BV-Cu	−0.2	5.4 ± 2.2	1.5 ± 0.9	3.21 ± 0.10
	0.2	4.0 ± 0.4	5.0 ± 0.9	3.15 ± 0.16
	0.6	3.6 ± 0.2	5.2 ± 1.1	3.66 ± 0.14

systems, but the Cl content increases with the higher potentials, reaching a contribution of 22.5% at the copper electrode in the chloride solution. There is a significant reduction in the concentration of chloride-containing species in the presence of the BV, particularly at the higher applied potentials, with the Cl values ranging from 3.6% to 5.4% and furthermore these compositions are independent of the potential. The C content increases as the potential is increased which suggests that although the BV is adsorbed onto the copper at −0.20 V vs SCE, slightly higher amounts are incorporated as the potential is increased. The presence of the viologen at the surface seems to stabilise the initial CuCl complex layer that is formed at −0.20 V vs SCE and very little chloride is further incorporated or deposited at the surface.

In order to determine if the BV-modified layer was retained at the surface when the copper was removed from the BV-containing solution, the BV-modified copper was well rinsed and placed in 0.1 M NaCl under open-circuit conditions for 30 min. Then the BV-modified copper was cycled in 0.1 M NaCl without the presence of the viologen in solution and in an electrochemical window where the viologen can be reduced. The voltammetry of this BV-modified copper and unmodified copper in a neutral 0.1 M NaCl solution, is shown in Fig. 4(a), where the redox chemistry of the viologen is clearly evident. The voltammogram of the deposited viologen is similar to the redox reactions of BV in solution recorded at a gold electrode, shown in Fig. 4(b). The two reduction peaks correspond to the two consecutive one-electron reductions, shown in Scheme 1, where the peak at −0.57 V vs SCE leads to the generation of the radical species, while the peak at −0.73 V vs SCE shows the conversion of the radical to the neutral compound [27]. On plotting the logarithm of the peak current for the reduction of the radical

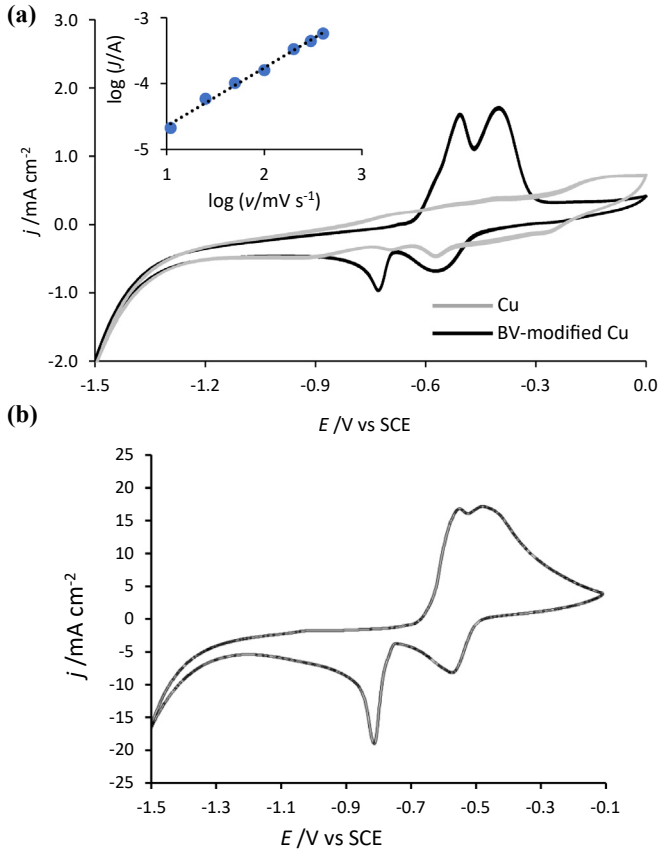

Fig. 4. Cyclic voltammograms recorded at 50 mV s^{-1} in 0.1 M NaCl for **(a)** copper (grey trace) and BV-modified copper (black trace) and **(b)** at a gold electrode in the presence of 5 mM BV^{2+} in solution. Inset shows the logarithm of peak current at −0.73 V vs SCE as a function of the logarithm of scan rate.

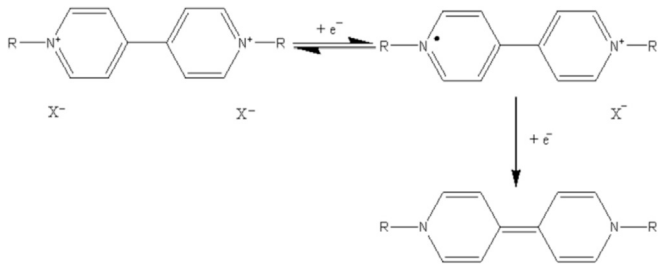

Scheme 1. Reduction of BV, where R is $CH_2C_6H_5$.

cation to the neutral species, at −0.73 V vs SCE, as a function of the logarithm of the scan rate, a linear plot was observed with a slope of 0.88, as illustrated in the inset in Fig. 4(a). This peak exhibits electrochemistry typical of an adsorbed species. However, slopes nearer to 0.50 were seen with the other peaks giving behavior closer to diffusion-controlled processes. This shows that the deposited BV is redox active and undergoes its characteristic reduction/oxidation reactions.

An estimation of the surface coverage of adsorbed BV was made using Eq. (3), where Γ represents the surface coverage, n represents the number of electrons transferred, A is the surface area, F is the Faraday constant and Q corresponds to the charge. The charge of the first reduction peak, corresponding to the conversion of BV^{2+} to $BV^{+\bullet}$, was computed by cycling the BV-modified electrode in 0.1 M NaCl after equilibration at open-circuit conditions for 30 min. This redox peak was chosen as the second reduction wave gives rise to the formation of BV^{o} which has limited solubility in aqueous solution.

$$\Gamma = \frac{Q}{nFA} \quad (3)$$

Using this approach, the surface coverage was computed as 1.87×10^{-6} mol cm^{-2} giving approximately 1.12×10^{18} molecules cm^{-2}.

3.2. Protective properties of the viologens

The protective properties of the BV-modified copper were studied in a neutral 0.10 M NaCl solution (not deoxygenated). Slow scan voltammograms were recorded, where the potential was cycled from −0.20 V to 1.0 V vs SCE at a scan rate of 1 mV s^{-1}. Representative data are presented in Fig. 5, where the BV-modified copper, the previously cycled BV-modified copper and uncoated copper are compared, with the current potential plots shown in Fig. 5(a) and the corresponding charge-potential plots presented in Fig. 5(b). It is clear from these data that very good stability is achieved with the BV-modified copper electrode. There is no evidence of significant copper dissolution, which is seen with the unmodified copper, and relatively low currents are maintained, Fig. 5(a), and while the charge increases somewhat at higher potentials, it remains significantly lower than that observed with the unmodified copper. After cycling the BV-modified copper in 0.1 M NaCl, the electrode was immersed in 0.1 M NaCl for 20 min and then polarised for a second time in the NaCl solution, to give the previously cycled BV-modified copper. Somewhat more dissolution was evident with this system, suggesting that the BV-modified copper electrode is altered when cycled to 1.0 V vs SCE in 0.1 M NaCl and these alterations reduce the protective properties. However, the freshly prepared BV-containing films show good protective properties. This is also evident in Fig. 6, where current-time plots are shown for the BV-modified copper polarised at 0.30 V and 0.60 V vs SCE in 0.1 M NaCl. Steady-state currents of approximately 5.0 and 10.0 μA cm^{-2} are observed at 0.30 V and 0.60 V vs SCE, respectively, indicating good stability.

The concentrations of Cu^{2+} dissolved from the unmodified and BV-modified copper electrodes polarised at −0.20 V, 0.30 V and 0.60 V vs SCE in 0.1 M NaCl for 30 min are summarised in Table 1. It is evident that lower concentrations of dissolved Cu^{2+} ions are seen with the BV-modified copper, while in both cases the application of higher potentials gives rise to increasing amounts of dissolved copper. However, the concentrations of copper in solution will be lower than the true values as the deposition of corrosion products, particularly at the unmodified copper electrode, evident in Fig. 1(a), will reduce and limit the release of copper into the solution. This was less evident with the BV-modified films as fewer corrosion products were deposited at the surface.

Typical polarisation plots are shown for pure copper and the BV-modified copper in Fig. 7, where it is clear that the BV-modified copper has a higher corrosion potential and a lower corrosion current. These data were further analysed by applying the Tafel equation, Eq. (4), which represents a single redox reaction, to the corrosion reaction, which involves two-half reactions. In this case, the oxidation-half reaction is the oxidation of copper, while the reduction-half reaction, corresponds mainly to the reduction of dissolved oxygen. As a result, the Tafel equation is modified to give Eq. (5). In this analysis, η is the overpotential, j is the measured current density, j_o represents the exchange current density, α is the transfer coefficient, E_{corr} is the corrosion potential and j_{corr} gives the corrosion current density, F corresponds to Faraday's constant, and

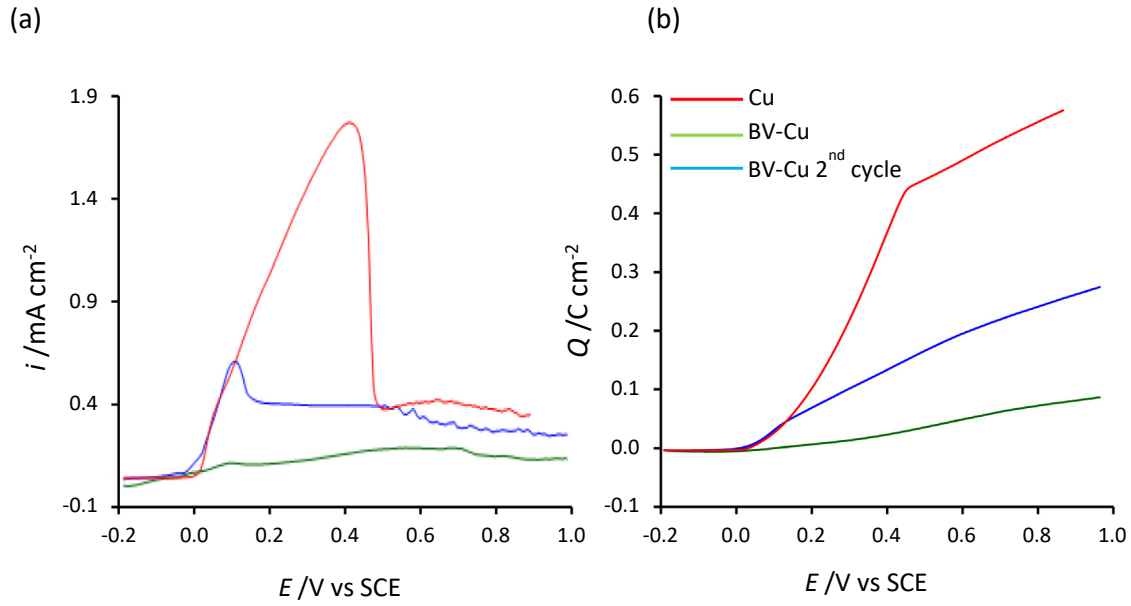

Fig. 5. **(a)** Slow scan voltammograms and **(b)** corresponding charge-potential plots, recorded at 1 mV s^{-1}, in 0.1 M NaCl for pure copper (red trace), BV-modified copper (green trace) and previously cycled BV-modified copper (blue trace).

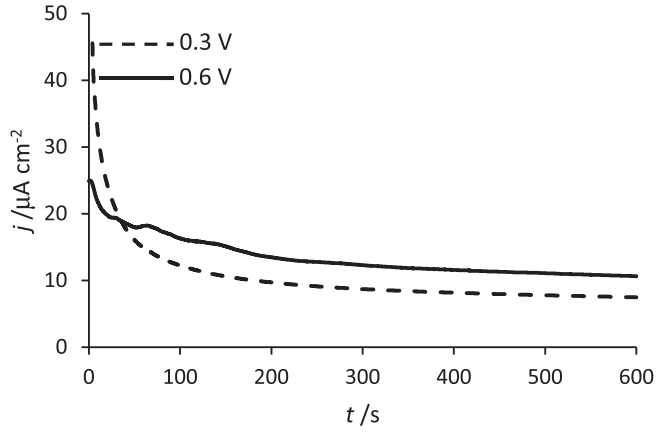

Fig. 6. Current-time plots recorded for BV-modified copper at ▬▬0.6 V and ▬ ▬ ▬0.3 V vs SCE in 0.1 M NaCl.

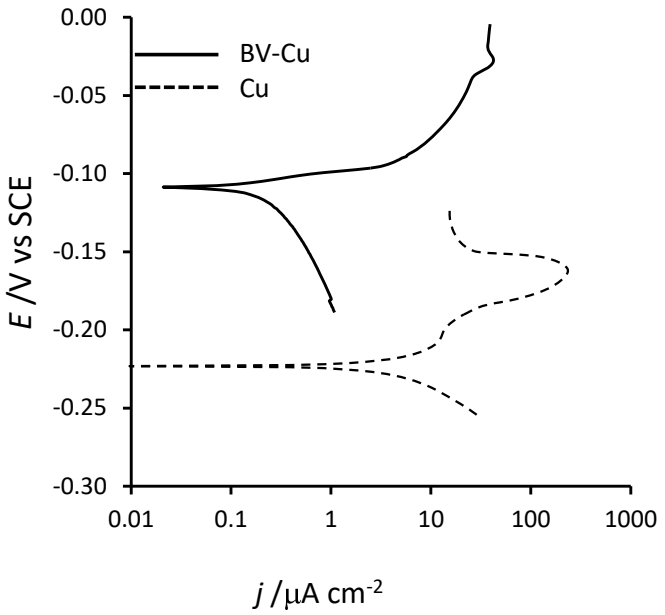

Fig. 7. Tafel plots recorded at 0.5 mV s^{-1} in 0.1 M NaCl for ▬▬BV-modified copper and ▬ ▬ ▬un-coated copper.

R is the gas constant. These fitted data are summarised in Table 2. For comparative purposes, data are provided for benzotriazole (BTA), which is a well-known solution inhibitor in the corrosion protection of copper [28,29]. It is clear from these data that the BV-modified copper compares very well with the corrosion inhibition seen with the BTA in solution. There is a clear reduction in the corrosion current density when the BV-modified copper is compared with the unmodified copper electrode. The lower corrosion current density and higher corrosion potential, seen with the BV-modified copper, are consistent with a reduction in the rate of the copper dissolution reaction. This is also in good agreement with the data presented in Fig. 5 where the BV-modified copper clearly minimises the dissolution of the copper substrate.

$$\eta = \frac{2.303RT}{\alpha F} log j_o - \frac{2.303RT}{\alpha F} log j \quad (4)$$

$$E - E_{corr} = \frac{2.303RT}{\alpha F} log j_{corr} - \frac{2.303RT}{\alpha F} log j \quad (5)$$

Electrochemical impedance spectroscopy (EIS) was also used to investigate and compare the properties and stability of the BV-modified copper with copper. The impedance response for BV-coated copper is shown in Fig. 8(a) at an applied potential of −0.15 V vs SCE. This potential was selected as both copper and the BV-coated copper are stable under these conditions. The impedance data were fitted to the equivalent circuit, shown in the inset, using a non-linear-least-squares fitting method. In this circuit, R_s represents the solution resistance, R_1 represents the charge-transfer resistance, while CPE_1 and CPE_2 are constant phase elements. The constant phase elements were used to determine the capacitance of the interface and also to model the diffusional

Table 2
Summary of Tafel analysis for copper, BV-modified copper and copper with BTA in solution.

System	b_a/mV decade^{-1}	b_c/mV decade^{-1}	E_{corr}/V vs SCE	j_{corr}/μA cm^{-2}
Un-coated Cu	54	89	−0.225 ± 0.015	1.85 ± 0.07
BV-Cu	83	94	−0.104 ± 0.025	0.89 ± 0.10
BTA in solution	57	72	−0.165 ± 0.017	1.14 ± 0.06

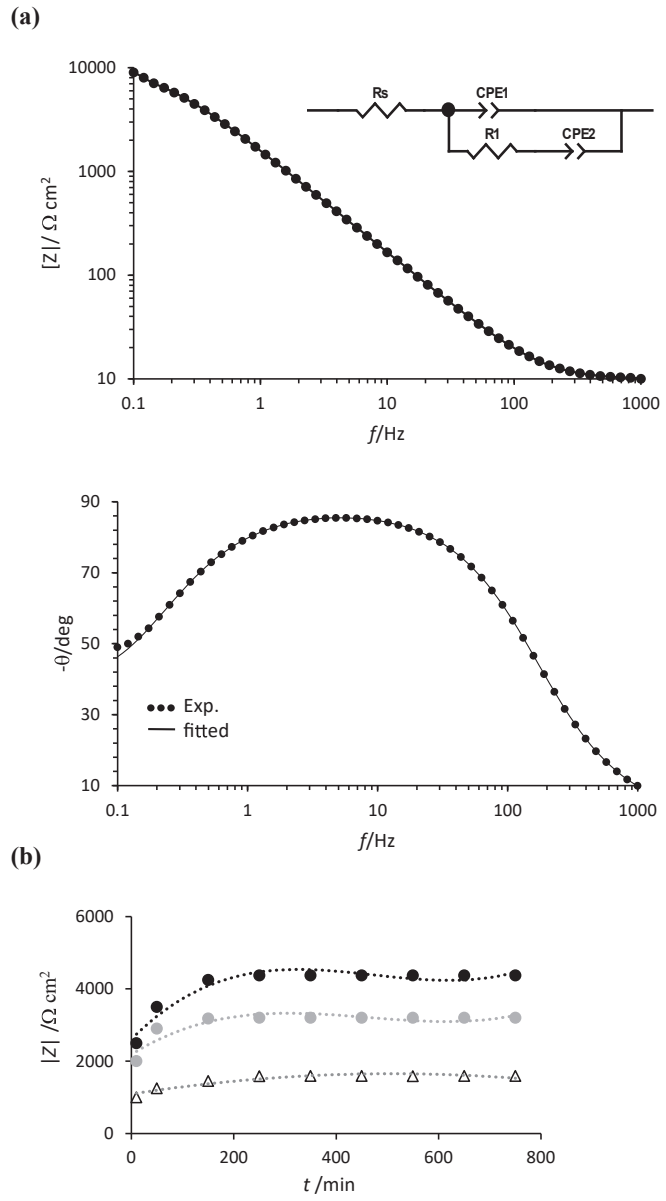

Fig. 8. **(a)** Impedance data recorded for BV-modified copper at −0.15 V vs SCE in 0.1 M NaCl, inset shows the equivalent circuit **(b)** charge-transfer resistance, R1, plotted as a function of time for BV-modified copper polarised at Δ 0.0 V ● 0.20 V and ●0.60 V vs SCE in 0.1 M NaCl.

processes. These were used rather than pure capacitors to take into account the inhomogeneity of the surface of the electrode. The impedance of a constant phase element, Z_{CPE} is defined in Eq. (6), with the fractional exponent, n, having values between 0 and 1.0 [30]. Here, j is the imaginary number, ω is the angular frequency and n represents a phase shift that is a measure of surface inhomogeneity. The fitted impedance data are summarised in Table 3, where n_2 is the fractional exponent of CPE2 and n_1 is used to represent the exponent of CPE1.

$$Z_{CPE} = {}^{1}/_{Q(j\omega)^n} \quad 6$$

For the BV-modified copper, R_1 represents the resistance of the viologen film and the resistance of the initial CuCl layer formed on copper prior to the deposition of the viologen, while CPE_1 corresponds approximately to the capacitance of the film, with an exponent close to unity ($n_1 = 0.87$). The capacitance was computed as 120 μF cm^{-2} and this remained constant over a 720 min-period. A slightly lower capacitance of 40 μF cm^{-2} ($n_1 = 0.83$) was obtained for the unmodified copper. The increase in the capacitance of the BV-modified copper is probably related to the charged $BV^{2+}2Cl^-$ layer at the surface. The resistance, R_1, was calculated as 8 kΩ cm^2, for the BV-modified copper and again there was little change in this resistance with continued polarisation. A higher resistance was calculated for the uncoated copper and this resistance varied from 21.2 kΩ cm^2 at 60 min to 14.5 kΩ cm^2 at 300 min. In addition, a clear diffusional term with an exponent close to 0.52 was observed for the uncoated copper, consistent with diffusional processes across the porous chloride film formed at the unmodified copper. This is consistent with the EDX data, shown in Table 1, where a relatively high chloride content is observed for the unmodified copper, giving a porous layer.

The charge-transfer resistance, R_1, for the BV-modified copper is plotted as a function of the polarisation period and shown in Fig. 8(b) at different applied potentials. Steady-state conditions are achieved after approximately 200 min and then the resistance remains constant with no evidence of further modification of the film or dissolution of copper from the underlying substrate. These data clearly show that the BV film has protective properties.

4. Conclusion

A Benzyl viologen (BV) layer was deposited at copper in an acidified 0.1 M NaCl solution to give a protective layer that inhibited the dissolution of copper. The viologen layer was formed following the dissolution of copper, to give a chloride layer, CuCl, that facilitated the formation of the viologen layer at the surface. Once the BV was deposited, it appeared to stabilise the underlying CuCl or adsorbed chloride layer and there was no evidence for the accumulation of further amounts of CuCl on immersion or polarisation in NaCl. The deposited BV exhibited redox behavior and was reduced to the radical cation at −0.57 V vs SCE and reduced further to the neutral molecule at −0.73 V vs SCE in 0.1 M NaCl, with the voltammograms recorded for the adsorbed BV being similar to that observed for the electrochemistry of BV dissolved in the solution phase at an inert gold electrode. The deposited BV provided a layer that inhibited the dissolution and corrosion of copper with the modified copper giving lower corrosion currents compared to the unmodified electrode. The protective properties were attributed to the enhanced stability of the initial BV-modified CuCl layer. While this layer may not be sufficiently stable for long-term corrosion protection in aggressive solutions, viologens are known to possess antibacterial properties and it may have applications as a component of a more complex coating system.

Table 3
Summary of impedance data for pure copper and BV-modified copper in 0.1 M NaCl.

Time/min	Copper				BV-modified Copper			
	$CPE_1/\mu F\ cm^{-2}$	$R_1/k\Omega\ cm^2$	$CPE_2/m\Omega^{-1}s^{n2}$	n_2	$CPE_1/\mu F\ cm^{-2}$	$R_1/k\Omega\ cm^2$	$CPE_2/m\Omega^{-1}s^{n2}$	n_2
60	38	21	1.77	0.4	120	8.10	0.05	0.7
180	40	18	1.71	0.5	128	8.12	0.05	0.7
300	41	14	1.66	0.5	130	8.15	0.05	0.7

Declaration of competing interest

The authors declare that they have no known competing financial interests or personal relationships that could have appeared to influence the work reported in this paper.

CRediT authorship contribution statement

Ursula Carragher: Investigation, Methodology, Writing - original draft. **Carmel B. Breslin:** Conceptualization, Methodology, Writing - review & editing.

Acknowledgements

The authors acknowledge funding from the Research Frontiers Programme, Science Foundation Ireland, RFP/MTR1261.

References

[1] P.D. Hale, L.I. Boguslavsky, H.I. Karan, H.L. Lan, H.S. Lee, Y. Okamoto, T.A. Skotheim, Investigation of viologen derivatives as electron-transfer mediators in amperometric glucose sensors, Anal. Chim. Acta 248 (1991) 155–161.
[2] L. Striepe, T. Baumgartner, Viologens and their application as functional materials, Chem. Eur J. 23 (2017) 16924–16940.
[3] S. Cosnier, B. Galland, C. Innocent, New electropolymerisable amphiphilic viologens for the immobilisation and electrical wiring of a nitrate reductase, J. Electroanal. Chem. 433 (1997) 113–119.
[4] S.K. Cook, B.R. Horrocks, Heterogeneous electron-transfer rates for the reduction of viologen derivatives at platinum and bismuth electrodes in acetonitrile, ChemElectroChem 4 (2017) 320–331.
[5] B. Cheng, A.E. Kaifer, Electrochemistry of viologen dications in cholate media and competition between the cholate assemblies and the cucurbit [7] uril host, Langmuir 31 (2015) 2997–3002.
[6] C.L. Bird, A.T. Kuhn, Electrochemistry of viologens, Chem. Soc. Rev. 10 (1981) 49–82.
[7] D.Y. Lee, A.K.M. Kafi, S.H. Park, Y.S. Kwon, Charge transfer property of self-assembled viologen derivative by electrochemical quartz crystal microbalance response, J. Nanosci. Nanotechnol. 6 (2006) 3657–3660.
[8] K. Arihara, F. Kitamura, Adsorption states of heptyl viologen on an Au(111) electrode surface studied by infrared reflection absorption spectroscopy, J. Electroanal. Chem. 550–551 (2003) 149–159.
[9] T. Higashi, T. Kawamoto, S. Yoshimoto, T. Sagara, Two sharp phase change processes of diphenyl viologen at a Au(111) electrode surface: non-Faradaic transition with interplay of ionic adsorption of chloride and bromide and Faradaic one, J. Phys. Chem. C 119 (2015) 1320–1329.
[10] M. Jiang, E. Sak, K. Gentz, A. Krupski, K. Wandelt, Redox activity and structural transition of heptyl viologen adlayers on Cu(100), ChemPhysChem 11 (2010) 1542–1549.
[11] S. Breuer, D.T. Pham, S. Huemann, K. Gentz, C. Zoerlein, R. Hunger, K. Wandelt, P. Broekmann, Organic layers at metal/electrolyte interfaces: molecular structure and reactivity of viologen monolayers, New J. Phys. 10 (2008) no.
[12] S.-L. Tsay, J.-S. Tsay, T.-Y. Fu, P. Broekmann, T. Sagara, K. Wandelt, Molecular structures of dicarboxylated viologens on a Cu(100) surface during an ongoing charge transfer reaction, Phys. Chem. Chem. Phys. 12 (2010) 14950–14959.
[13] D.T. Pham, K. Gentz, C. Zoerlein, N.T.M. Hai, S.L. Tsay, B. Kirchner, S. Kossmann, K. Wandelt, P. Broekmann, Surface redox chemistry of adsorbed viologens, New J. Chem. 30 (2006) 1439–1451.
[14] T. Higashi, T. Sagara, Remarkable effect of bromide ion upon two-dimensional faradaic phase transistion of dibenzyl viologen on an Hopg electrode surface: emerge of two step transition, Electrochim. Acta 114 (2013) 105–115.
[15] T.H. Phan, K. Wandelt, Molecular self-assembly at metal-electrolyte interfaces, Int. J. Mol. Sci. 14 (2013) 4498–4524.
[16] B.-Y. Wen, J. Yi, Y.-H. Wang, K. Madasamy, H. Zhang, M. Kathiresan, J.-F. Li, Z.-Q. Tian, In-situ monitoring of redox proceses of viologen at Au(hkl) single-crystal electrodes using electrochemical shell-isolated nanoparticle-enhanced Raman spectroscopy, Electrochem. Commun. 72 (2016) 131–134.
[17] M.D. Peterson, S.C. Jensen, D.J. Weinberg, E.A. Weiss, Mechanisms for adsorption of methyl viologen on CdS quantum Dots, ACS Nano 8 (2014) 2826–2837.
[18] R.R. Kashapov, Y.S. Razuvayeva, A.Y. Ziganshina, R.K. Mukhitova, A.S. Sapunova, A.D. Voloshina, L.Y. Zakharova, Self-assembling and biological properties of single-chain dicationic pyridinium-based surfactants, Colloids Surf., B 175 (2019) 351–357.
[19] S.J. Yuan, F.J. Xu, E.T. Kang, S.O. Pehkonen, Modification of surface-oxidised copper alloy by coupling of viologens for inhibiting microbiologically influenced corrosion, J. Electrochem. Soc. 154 (2007) C645–C657.
[20] H.-H.Strehblow V. Maurice, P. Marcus, Initial and later stages of anodic oxide formation on Cu, chemical aspects, structure and electronic properties, Electrochim, Acta 46 (2001) 3755–3766.
[21] H. Tian, Y.F. Cheng, W. Li, B. Hou, Triazolyl-acylhydrazone derivatives as novel inhibitors for copper corrosion in chloride solutions, Corrosion Sci. 100 (2015) 341–352.
[22] A.D. Modestov, G.-D. Zhou, Y.-P. Wu, T. Notoya, D.P. Schweinsberg, A study of the electrochemical formation of Cu(I)-BTA films on copper electrodes and the mechanism of copper corrosion inhibition in aqueous chloride/benzotriazole solutions, Corrosion Sci. 36 (1994) 1931–1946.
[23] J.Y. Josefowicz, L. Xie, G.C. Farrington, Observation of intermediate cuprous chloride species during the anodic dissolution of copper using atomic force microscopy, J. Phys. Chem. 97 (1993) 11995–11998.
[24] C. Gouveia-Caridade, A. Romeiro, C.M.A. Brett, Electrochemical and morphological characterisation of polyphenazine films on copper, Appl. Surf. Sci. 285 (2013) 380–388.
[25] A.M. Fenelon, C.B. Breslin, Corrosion protection properties afforded by an in-situ electropolymerized polypyrrole layer on CuZn, J. Electrochem. Soc. 150 (2003) B540–B546.
[26] A.M. Fenelon, C.B. Breslin, The electropolymerization of pyrrole at a CuNi electrode: corrosion protection properties, Corros, Science 45 (2003) 2837–2850.
[27] V. Annibaldi, C.B. Breslin, Electrochemistry of viologens at polypyrrole doped with sulfonated β–cyclodextrin, J. Electroanal. Chem. 832 (2019) 399–407.
[28] O. Geuli, D. Mandler, The synergistic effect of benzotriazole and trimethylsiloxysilicate towards corrosion protection of printed Cu-based electronics, Corrosion Sci. 143 (2018) 329–336.
[29] A.M. Fenelon, C.B. Breslin, An electrochemical study of the formation of benzotriazole surface films on copper, zinc and a copper-zinc alloy, J. Appl. Electrochem. 31 (2001) 509–516.
[30] E. Barsoukov, J. Macdonald, in: E. Barsoukov, J. Macdonald (Eds.), Impedance Spectroscopy: Theory, Experiment, and Applications, second ed., John Wiley and Sons, 2005.